3D Modeling of Contact Problems and Hysteresis in Coupled Electro-Mechanics

J.R. Gilbert, G.K. Ananthasuresh, and S.D. Senturia
Microsystems Technology Laboratories, M.I.T., Cambridge, MA. 02139

ABSTRACT

This paper discusses the modeling of electro-mechanical hysteresis in devices which exhibit contact between components. We make use of a recently developed tool, CoSolve-EM, in order to solve quasi-static 3D contact electro-mechanics for a clamped - clamped beam, calculating full displacement, capacitance and contact force vs. voltage. We then extend the simulations to two design variations of the beam which permit engineering of its hysteresis characteristics.

INTRODUCTION

Micro-electro-mechanical systems (MEMS) are usually designed on scales at which electrostatic forces are capable of moving or deforming the parts of the device. In this regime accurate prediction of device behavior requires the solution of coupled problems involving electrostatic and mechanical and/or elastic energy. One interesting class of MEMS, including relays [1], distributed linear actuators [2], stepping actuators [3], curved electrode actuators [4,5], zipping actuators [6], micromirrors [7,8,9,10,11], micromotors [12] and valves [13], contain a movable part which touches down or "contacts" a fixed surface in the course of the device's normal operation. These devices can exhibit electro-mechanical hysteresis. In some cases such hysteresis might be viewed as a defect to be avoided, in others a feature to be designed for exploitation [14]. Some sensor designs make use of the contact phenomenon to alleviate the nonlinearity of the capacitance vs. the input signal characteristic and also improve the sensitivity of the device (e.g., the touch-down-mode pressure sensor [15,16]).

The devices of the types mentioned above, depending on their application, may require accurate prediction of the transition voltages at which the structure makes contact and is released, as well as the variation of capacitance and contact force. Electromechanical contact problems can be analytically modeled if the structure has regular geometry with sufficient symmetry [15]. For other types of structures, numerical solution methods, such as finite element (FE) or boundary element (BE) techniques, are needed. Some work in 3D FE modeling of contact electro-mechanics has been done using the parallel plate approximation for the electrostatic domain [17], and we have previously reported some success using coupled FE/BE methods for contact problems [18]. Several groups have recently been working on tools for general coupled electromechanics problems [19,20].

In this paper we extend the analysis of electromechanical hysteresis to full 3D in both the elastic and electrostatic domains. As an illustrative example we discuss the analysis of a doubly clamped beam pulled in against a ground plane. We show the results for predicting pull-in, release, capacitance, contact force, and the systemic hysteresis that this class of devices are subject to. We make use here of our recently developed package, CoSolve-EM [18], a coupled solver for quasi-static electro-mechanics, which enables the 3D numerical analysis of this class of devices. We then demonstrate the use of the simulator to explore the consequences of some design perturbations of the basic beam model.

0-7803-2985-6/96 $5.00 © 1996 IEEE

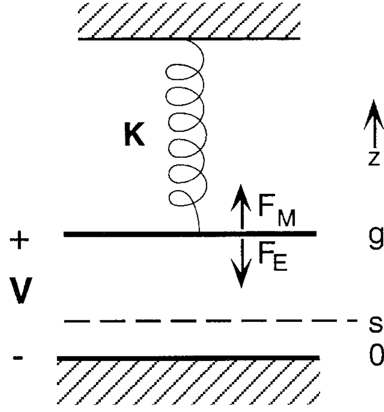

Figure 1. Sketch of the 1D model. F_E is the electrostatic actuating force, F_M is elastic restoring force. The fixed plate is at z=0, the moveable plate starts at z=g, and the contact surface is at z=s.

ELECTROMECHANICAL HYSTERESIS

The basic features of electro-mechanical hysteresis are evident even in the simplest one dimensional model shown in Figure 1. This model is essentially a parallel-plate capacitor of area, A with a fixed ground plate, and a moving plate restrained by a linear spring of known stiffness, K. There is a rigid stop at a distance s above the ground plane (the dashed line in the figure) which corresponds to an insulating layer on the ground electrode in actual devices.

The force balance equation for this model can be written, as in equation (1), by summing together the actuating nonlinear electrostatic force, F_E, and the linear restoring force due to the spring, F_M.

$$0 = F_M + F_E = K(g-z) - \frac{\varepsilon_0 A}{2z^2} V^2 \qquad (1)$$

If we start the device at its undeformed position (z=g, in Figure 1), we can turn V on slowly (slow enough to neglect inertia), and find stable solutions for the plate position until a critical voltage, the pull-in voltage, V_{PI}, is reached. At V_{PI}, the $1/z^2$ growth of the electrostatic force becomes dominant over the linearly increasing mechanical restoring force, and the device pulls in, stopping at z=s. In this 1D model the pull-in occurs when the plate reaches a position z=2g/3 for a quasi-statically applied voltage. If, instead, we start with the device displaced to touch the contact surface at s, we have stable solutions at z=s, for all $V>V_R$, the release voltage. The release voltage may be defined as the voltage at which the electrostatic force exactly balances the spring force of the pulled in plate. If $V_R < V_{PI}$, the system has two valid solutions over the same band of voltages, and is capable of exhibiting hysteresis. The condition $V_R < V_{PI}$ implies that the location of the stopping plane is below 2g/3.

To simulate the same beam to be discussed below using this 1-D model, we used plate area A = 800μm^2 and spring constant K= 16N/m, and so obtained the dashed hysteresis curve shown in Figure 2.

The curve shows the simulated response of the system to (slowly) ramping the voltage from 0V to above V_{PI} and back to 0V. The pull-in and release voltages are respectively 15V and 5V for this 1D model.

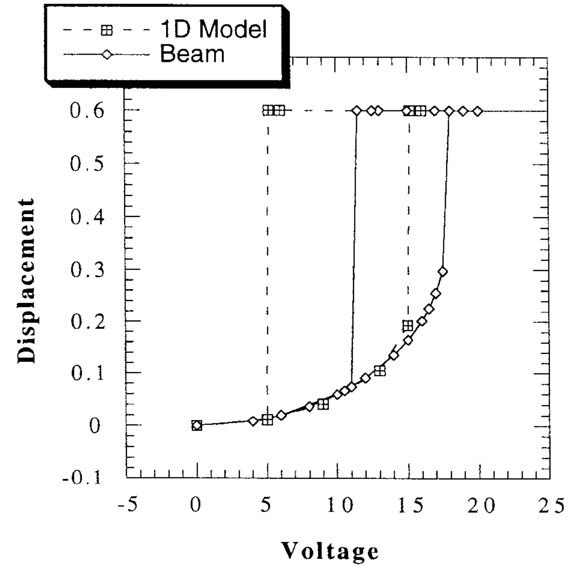

Figure 2. Displacement vs. voltage for the 1D model and the 3D beam. For the 3D electromechanical solver, displacement is the maximally displaced node in the model, in this case, at the center of the beam. For the 1D model, V_{PI} = 15V and V_R=5V. For the beam, $17.5V<V_{PI}<18.0V$, and $11.0V < V_R < 11.5V$.

The 1D model uses a single spring constant for the entire device behavior, and neglects the distributed capacitance of the deformed beam. It also neglects all fringing effects in the electrostatic analysis.

TOOLS AND METHODS FOR THE 3D PROBLEM

CoSolve-EM is a Coupled Solver for Electro-Mechanics. It finds the self-consistent solution to electro-mechanical problems using an external, boundary-based coupling between a mechanical FE solver (ABAQUS [21]) and an electrostatic BE solver (FASTCAP [22]), implementing both relaxation and SNGCR (Surface Newton - Generalized Conjugate Residual) techniques for convergence [23]. CoSolve-EM is a package that we have been developing for several years. An overview of some of its applications was given at MEMS 1995 [18]. In this paper we describe its use for 3D electromechanical contact problems with hysteresis.

CoSolve-EM can be used to find an estimate for pull-in or release voltages in the following manner. We solve for the coupled solution of the problem at every voltage of a sequence and observe that the device has not pulled in at V_i but has pulled-in at V_{i+1}. We then estimate $V_i < V_{PI} < V_{i+1}$. We can, of course choose sequences to get us any desired accuracy, at some computational cost, and CoSolve-EM does automate this process. When we plot curves of displacement vs. voltage these curves will show a line of finite slope over the jumps of pull-in or release. This line gives the bounds on the V_{PI} or V_R step. In Figure 2 the pull-in for the beam model takes place between 17.5V and 18.0V, and the curve shows a segment of finite slope there, instead of the vertical line that we expect from the underlying physics.

A BEAM UNDER ELECTROSTATIC LOAD

Consider the model problem of a beam, clamped at either end, suspended 0.7μm over a ground plane, with a contact stop at 0.1μm above the ground plane. The beam has length L = 80μm, width W = 10μm, and thickness T = 0.5μm. It has material properties, E = 169GPa, ν = 0.25, and negligible residual stress.

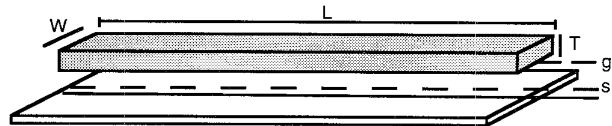

Figure 3. Sketch of the model beam, L=80μm, W=10μm, T=0.5μm, gap g=0.7μm, and the stop s=0.1μm. The ground plane is at z=0.

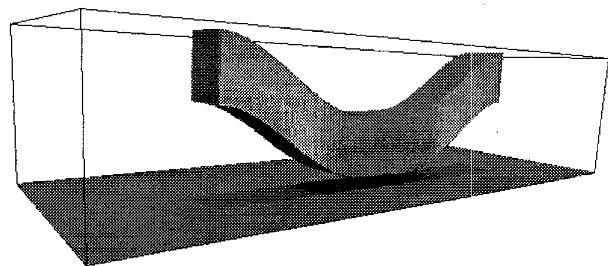

Figure 4. 3D view of the deformation of the beam at 20V. The view shows shading on the ground plane representing the image charge induced there. The z scale is exaggerated by a factor of 25.

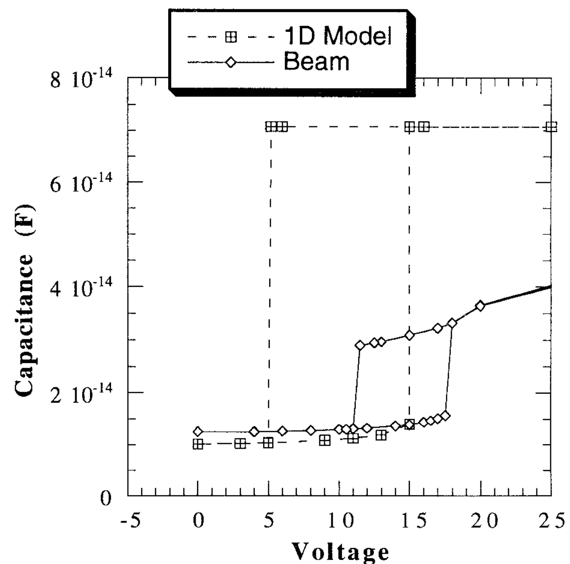

Figure 5. Capacitance vs. voltage for the 1D model and the 3D beam. The 1D model is overestimating the touchdown capacitance.

Figure 3 shows a sketch of such a beam A voltage is applied between the beam and the ground plane. Under such an electrostatic load the beam deflects down to the contact surface and deforms against it. The hysteresis of the displacement of the center of the beam is plotted in Figure 2. Figure 4 shows a 3D visualization of the beam deformed under 20V load.

Figure 2 shows that the 3D beam model exhibits the same qualitative hysteresis in displacement vs. voltage that we encountered in the 1D model.

The 1D and 3D models do show some differences because the 1D model ignores the deformation of the plate. Thus it overestimates the touchdown capacitance and underestimates the release voltage V_R.

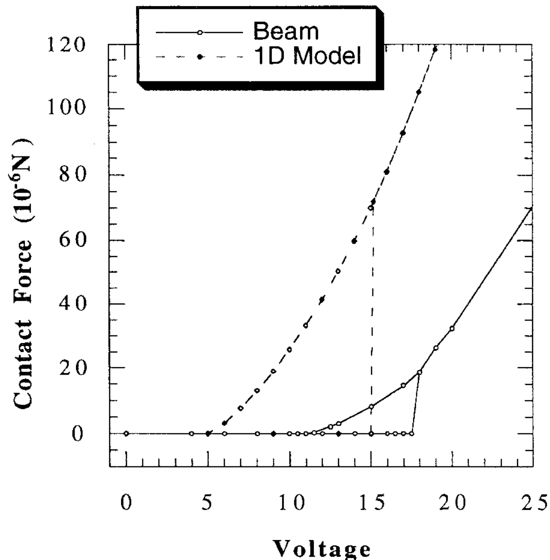

Figure 6. Contact force vs. voltage for the 1D model and the beam.

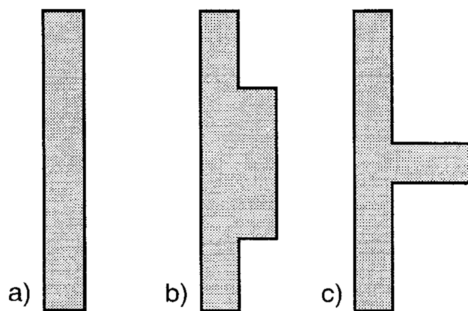

Figure 7. Top view of beams, (a) the basic beam. (b) wide flap (40 x 10). (c) the narrow flap (10 x 20). All in μm.

Design of applications such as sensors and mechanical actuators may also require the curves for capacitance vs. voltage and contact force vs. voltage. These curves are plotted in Figure 5 and Figure 6.

3D VARIATIONS OF THE BEAM

We can now perform some design experiments on the basic beam to manipulate its V_{PI} and V_R values. Figure 7 summarizes two variants of the beam that we have simulated. Both involve attaching an asymmetric flap to the beam. In Figure 7b we sketch a beam with a wide flap (40μm x 10μm) and in Figure 7c we sketch a beam with a narrow flap (10μm x 20μm). Both variants have the effect of lowering both the pull-in and the release voltages.

Figure 8 shows the displacement vs. increasing voltage for each of the beam variants. Figure 9 shows the displacement vs. decreasing voltage for each of the variants. In both sets of curves we can see that the design variants have shifted the pull-in and release voltages.

Figure 10 shows the capacitance vs. increasing voltage for each of the three variants. In this case the difference in V_{PI} between the beam and the beam with narrow flap appears reduced from what was observed in Figure 8. This is explained by the fact that the narrow flap touches down before the bulk of the beam itself. Figure 11 shows the 3D image of the bottom surfaces of the narrow flap beam at 11.5V (when the flap is just touching down). Figure 12 shows the same beam at 12.5V, after the center of the beam has been pulled down. In this example we are modeling the quasi-static version of the process of "zipping" discussed and demonstrated by several authors [4,5,6].

When we plot displacement, we are plotting the displacement of the maximally displaced point. In the case of the beam with narrow flap this point occurs at the tip of the narrow flap itself. When we plot capacitance, we are plotting a quantity more sensitive to the position of the bulk of the device. So as the

device goes from its position in Figure 11 to the one in Figure 12 the reported displacement does not change (the tip is already down) but the capacitance changes considerably.

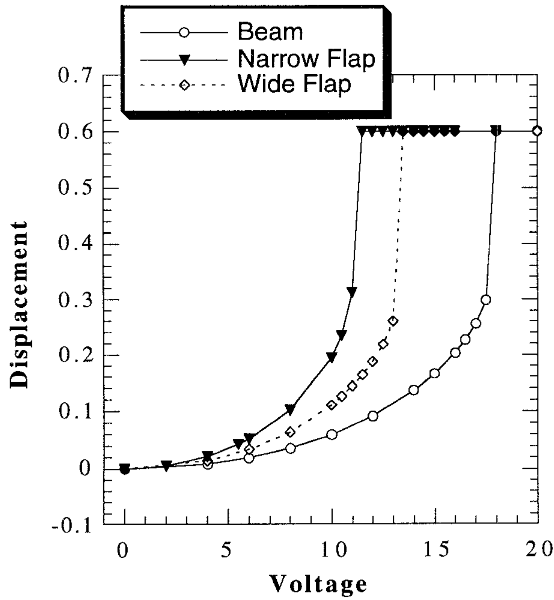

Figure 8. Displacement vs. increasing voltage for the variations of the beam

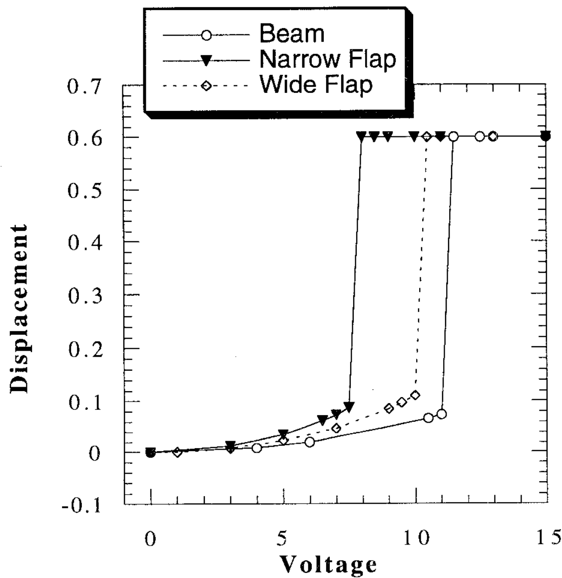

Figure 9. Displacement vs. decreasing voltage for each of the variations of the beam.

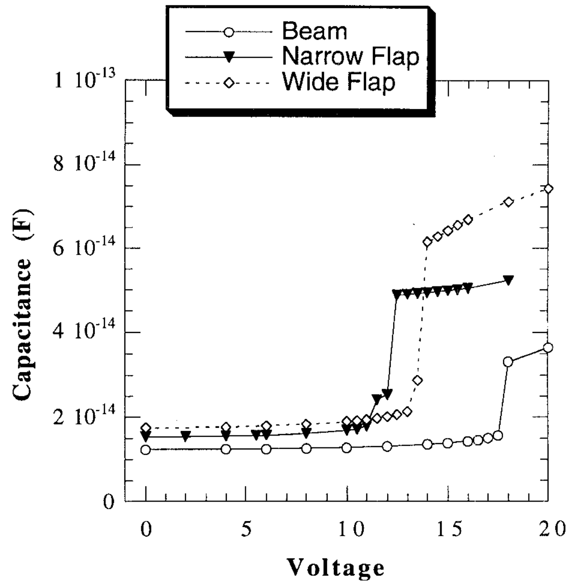

Figure 10. Capacitance vs. increasing voltage for each type of beam.

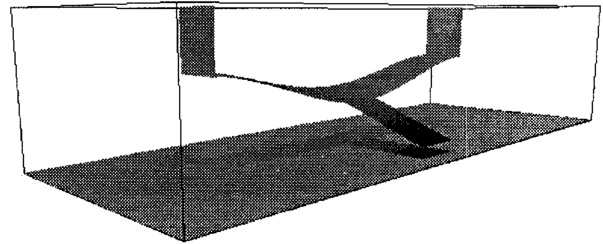

Figure 11. 3D view of the bottom surface of the beam with narrow flap at 11.5V, just after the initial touchdown of the flap tip. The figure is otherwise as in Figure 4.

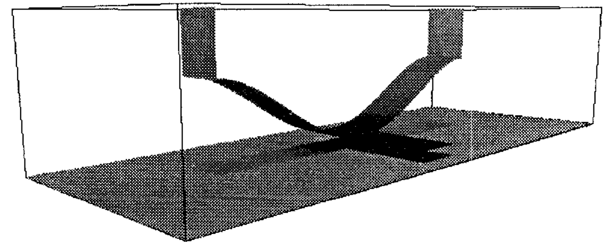

Figure 12. 3D view of the bottom surface of the beam with narrow flap at 12.5V, after the flap has pulled down the center of the beam. The figure is otherwise as in Figure 4.

CONCLUSION

The results reported here show that we can now perform full 3D analysis of contact electro-mechanics problems with hysteresis. Using CoSolve-EM, such problems can be solved from general meshed device descriptions, with no requirement to customize the modeler for each different type of geometry. This will enable MEMS designers to explore a wide design space of variations on interesting devices using software simulations.

ACKNOWLEDGMENTS

The CoSolve-EM package used in this paper has been developed over several years as part of the MEMCAD project at MIT. The work has been supported by DARPA contract J92-FBI-196 as well as equipment grants from Hewlett Packard and Digital Equipment. The authors would like to thank Jacob White and Rob Legtenberg for many valuable discussions and insights, as well as King Yu and Gregory Pal for their contributions to CoSolve-EM.

References

1 J. Drake, H. Jerman, B. Lutze, and M. Stuber, "An Electrostatically Actuated Micro-Relay", Proc. Transducers 95, Stockholm, paper no. 329-B10.

2 M. Yamaguchi and K. Kawamura, "Distributed Electrostatic Microactuator", Proc. MEMS 1993, Fort Lauderdale, FL, pp. 18-23.

3 T. Akiyama and K. Shono, "A New Step Motion of Polysilicon Microstructures", Proc. MEMS 1993, Fort Lauderdale, FL, pp. 272-277.

4 R. Legtenberg, et al., "Electrostatic Curved Electrode Actuator", Proc. MEMS 1995, Amsterdam, pp. 37-42.

5 Branedbjerg and Gravesen, "A New Electrostatic Actuator Providing Improved Stroke Length and Force", Proc. MEMS 1992, Travemünde, Germany, pp. 6-11.

6 K. Sato and M. Shikida, "Electrostatic Film Actuator with a Large Vertical Displacement", Proc. MEMS 1992, Travemünde, Germany, pp. 1-5.

7 V. P. Jaecklin, C. Linder, and N. F. de Rooij, "Optical Microshutters and Torsional Micromirrors for Light Modulation Arrays", Proc. MEMS 1993, Fort Lauderdale, FL, pp. 124-127.

8 J. B. Sampsell, "The Digital Micromirror Device and its Application to Projection Displays", Proc. Transducers 93, Yokohoma, pp. 24-27.

9 H. Toshiyoshi and H. Fujita, "An Electrostatically Operated Torsion Mirror for Optical Switching Device", Proc. Transducers 95, Stockholm, paper no. 68-B1.

10 H. Kück, W. Doleschal, A. Gehner, W. Grundke, R. Melcher, J. Paufler, R. Seltmann, and G. Zimmer, "Deformable Micromirror Devices as Phase Modulating High Resolution Light Valves", Proc. Transducers 95, Stockholm, paper no. 69-B1.

11 M. Fischer, M. Nägele, D. Echner, C. Schöllhorn, R. Strobel, "Integration of Surface Micromachined Polysilicon Mirrors and a Standard CMOS Process", Proc. Transducers 95, Stockholm, paper no. 70-B1.

12 R. Legtenberg, et al. "An Electrostatic Lower Stator Axial Gap Wobble Motor: Design and Fabrication", Proc. Transducers 95, Stockholm, paper no. 335-B11.

13 M. Huff, M. Mettner, T. Lober, and M. Schmidt, "A Pressure-Balanced Electrostatically-Actuated Microvalve", Proc. IEEE Solid State Sensor and Actuator Workshop, Hilton Head, SC, 1990, pp. 123-127.

14 R.B. Apte, F.S.A. Sandejas, W.C. Banyai, and D.M. Bloom, "Deformable Grating Light Valves for High Resolution Displays", Proc. IEEE Solid State Sensor and Actuator Workshop, Hilton Head, SC,1994, pp. 1-6.

15 X. Ding, L-J. Tong, W. He, J. Hsu, and W. Ko, "Touch-mode Silicon Capacitive Pressure Sensors", Microstructures, Sensors, and Actuators, ASME, DSC-Vol. 19. Edited by D. Cho et al., 1990, pp. 111-117.

16 L. Rosengren, J. Södeskvist, and L. Smith, "Micromachined Sensor Structures with Linear Capacitive Response", Sensors and Actuators A, Vol. 31, pp. 200-205 (1992).

17 B.E. Artz and L.W. Cathey, "A Finite Element Method for Determining Structural Displacements Resulting from Electrostatic Forces", Proc. IEEE Solid State Sensor and Actuator Workshop, Hilton Head, SC, 1992, pp 190-193.

18 J.R. Gilbert, R. Legtenberg, and S.D. Senturia, "3D Coupled Electro-Mechanics for MEMS: Applications of CoSolve-EM", Proc. MEMS 1995, Amsterdam, pp. 122-127.

19 H.U. Schwarzenbach, J.G. Korvink, M. Roos, G. Sartoris, and E. Anderheggen, "A micro electro mechanical CAD extension for SESES", J. Micromech. Microeng, Vol. 3, pp. 118-122 (1993).

20 U. Beerschwinger, et al., "Coupled Electrostatic and Mechanical FEA of a Micromotor", JMEMS, Vol. 3, pp 162-171 (1994).

21 ABAQUS Manual, Hibbitt, Karlsson & Sorenson, Inc. 1080 Main Street, Pawtucket, RI 02860, USA.

22 K. Nabors and J. White, "FastCap: A multipole-accelerated 3-D capacitance extraction program", IEEE Transactions on Computer-Aided Design, Vol. 10, pp. 1447-1459 (1991).

23 X. Cai, H. Yie, P. Osterberg, J. Gilbert, S. Senturia, and J. White, "A Relaxation/Multipole-Accelerated Scheme for Self-Consistent Electromechanical Analysis of Complex 3-D Microelectromechanical Structures", Proc. Int. Conf. on Computer-Aided Design, Santa Clara, CA, November 1993, pp. 270-274.